Thermal effect on structural and magnetic properties of Fe$_{78}$B$_{13}$Si$_9$ annealed amorphous ribbons

Mohamed Larbi Soltani[1,*], *Abdelhay* Touares[1], *Tiburce A.M.* Aboki[2], and *Jean-Georges* Gasser[3]

[1]LPS, Dpt. de Physique-Annaba University, Route d'El Hadjar BP 12 Annaba, Algérie
[2]GMS-LPCS UMR 7045, Chimie Paristech, 11 rue Pierre et Marie Curie, F-75231 Paris Cedex 05, France
[3]LCP –A2MC Institut de Chimie, Physique et Matériaux, Université de Lorraine, 1 bd Dominique François Arago 57078, Metz Cedex 3, France

Abstract. In the present work, we study the influence of thermal treatments on the magnetic properties of as-quenched and pre-crystallized Fe$_{78}$Si$_9$B$_{13}$ after stress relaxation. The crystallization behavior of amorphous and treated Fe$_{78}$Si$_9$B$_{13}$ ribbons was revisited. The measurements were carried out by means of Differential Scanning Calorimetry, by X-ray diffraction and by Vibrating Sample Magnetometer, Susceptometer and fluxmeter. Relaxed samples were heated in the resistivity device up to 700°C and annealed near the onset temperature about 420°C for respectively 1, 3, 5, 8 hours. In as-quenched samples, two transition points occur at about 505°C and 564°C but in relaxed sample, the transition points have been found about 552°C and 568°C. Kinetics of crystallization was deduced for all studied samples. Annealing of the as-purchased ribbon shows the occurrence of α-Fe and tetragonal Fe$_3$B resulting from the crystallization of the remaining amorphous phase. The effects on magnetic properties were pointed out by relating the structural evolution of the samples. The magnetic measurements show that annealing change the saturation magnetization and the coercive magnetic field values, hence destroying the good magnetic properties of the material. The heat treatment shows that the crystallization has greatly altered the shape of the cycles and moved the magnetic saturation point of the samples. The effect of treatment on the magneto-crystalline anisotropy is also demonstrated.

1 Introduction

To obtain nanocrystalline structure, different techniques are available; the crystallization method is an effective one. The basic idea is to control the crystal nucleation and growth during the crystallization process by empirical adjusting of the heat treatment conditions. As an example, the isothermal heat treatment at 450°C leads to complete crystallization of

_____

* Corresponding author: ml_soltani@yahoo.com

the amorphous Fe-B-Si in about 72 hours. By extrapolation, one can estimate that about 277 hours are required for the formation of nanograins of 400 nm size, as reported by [1]

The amorphous alloys based on Fe-B-Si are successfully applied as the core materials in distribution transformers due to their low core losses and relatively high saturation magnetization and low exciting current [2]. Therefore, it is necessary to determine both the conditions in which the properties of the as-received state of the metallic glass are conserved and the parameters of the kinetics of change. Knowledge of the crystallization kinetics of amorphous alloys offers the possibility for specific crystalline structures and hence for optimizing their properties. The elimination of both internal and external stresses improves the mobility of the Bloch walls of magnetic domains and facilitates reorientation of spins and magnetic saturation under an applied field H. Stress relaxation is observed by annealing the amorphous alloy at temperatures allowing sufficient atomic diffusion for structural relaxation but not enough to initiate crystallization [3]. The optimization of soft-magnetic properties of metallic glasses can be made by dynamical current annealing, One can obtain the structure relaxation, where the atoms rearrange to become more ordered with increasing annealing temperature, without bulk crystallization occurring. Authors reported that whereas there is no trace of crystalline phase for the samples annealed at 420°C, the as-quenched sample exhibits a broad peak from amorphous phase which is slightly larger than the corresponding peak of the relaxed sample, implying the occurrence of atomic rearrangement during annealing [4] Moreover, in the relaxed sample, the crystalline phase is still dispersed in the amorphous matrix and the small peak centered in the broad amorphous peak corresponds to α-Fe phase. The annealing effects on the thermomagnetic structural evolution of the $Fe_{78}B_{13}Si_9$ amorphous alloy have an effective disadvantage: the amorphous alloys such as Fe-B-Si are ductile in the as-cast state, but become brittle during conventional annealing [5]. After crystallization, the most attractive properties of an amorphous alloy, such as soft magnetic behavior, high strength, and ductility are usually lost. Thus, the limiting factor of many technological applications of nanocrystalline materials is their brittleness [6].

The magnetic saturation would depend on the internal stress states resulting from the as-cast conditions and further treatments of the alloy. Escobar *et* al. [3] have reported, also like Kronmüller quoted by Luborsky [7], the coercive field dependence on temperature [8]. H. Kronmüller, in [9], again pointed out that the defect concentration and fluctuations affect the magnetic properties of amorphous alloys. This behavior may be compared with the results of Escobar *et* a1. [3] who optimized the magnetic properties of Fe-Si-B alloys by a very short annealing at 430°C. But it seems that the absolute magnetic saturation of this alloy occurs at higher field in accordance with the work of Pankhurst et a1 [10], who using Mossbauer studies did not reach the saturation state for the same composition with applied field of up to 5T.

The aim of this study is to analyze the thermal, microstructural and magnetic properties of Fe-B-Si metallic glass. As-quenched alloys exhibit the typical macroscopic behavior of fully amorphous structures, while annealing induces, besides strain relaxation, moderate growth of the nanocrystals.

Quenched state (as-cast) and relaxed ribbons which exhibit in a dispersed α-Fe crystallites, have been investigated, particularly, in point of view of kinetics of crystallization of Fe-B-Si. The non-isothermal Differential Scanning Calorimetry (DSC) was used with the effect of annealing procedure on the structural and magnetic properties.

2 Experimental

Specimen used in this work are cut from ribbons approximately 25-µm thick and 10-mm wide wired, purchased from Allied Chemical Ltd (2605-S2). The amorphous ribbon, which has undergone structural relaxation by heat treatment at about 250° C, for a period of 2 hours, is referred to as a relaxed amorphous alloy.

This treatment is carried out immediately after rapid quenching by Allied Corp either without the application of a magnetic field or under magnetic field according to the requirement. In the case of this study, the magnetic field which allows uniaxial magnetic anisotropy is not applied. This structural relaxation makes it possible to reorganize the amorphous structure by relaxing the constraints due to rapid solidification.

Differential Scanning Calorimetry (DSC) measurements are used to study the thermal behavior. The METLER TOLEDO DSC 822^e apparatus is used. Amorphous and relaxed samples were continuously heated in the device to temperatures at which different crystallization stages could be obtained.

The measurements were carried out at continuous heating rates between 5 and 80 K/minute up to 700°C with accuracy of ±1°C, for as-quenched, relaxed, fully crystallized and isothermally annealed samples at different times. Heat treatment conditions were selected according to the beginning of the pre-crystallization process resulting from the first heating and cooling. At 420 °C, measurements are performed as function of time. This temperature is known to bring the optimum of magnetic quality (near Curie Temperature Tc ≈ 415°C). Crystalline phase's characterization was obtained by means of a Siemens D5000 diffractometer using Cu-Kα radiation. Susceptometer-3Tesla and VSM-9Tesla Quantum Design-PPMS (Physical Property Measurement System) were used for magnetic saturation measurements with high applied magnetic field up to 2 Tesla in order to saturate the as-received and 420°C-annealed samples.

To observe, in experiments, the dynamics of the walls in ferromagnetic one choose a Fluxmeter [11] for hysteresis loop measurements at variable amplitude. One connected a magnetic circuit like a transformer, by taking the values of magnetic applied field H (T) from primary circuit and magnetic induction B (T) from secondary circuit simultaneously.

3 Results and discussion

3.1 DSC results

The Differential Scanning Calorimetry DSC was used to study the crystallization kinetics of $Fe_{78}Si_9B_{13}$ glasses at the heating rates of 5, 20, 40 and 80K/m. Differential scanning calorimetry (DSC) measurements of the as-cast $Fe_{78}Si_9B_{13}$ metallic glass are presented in Figure 1. In each DSC curve, two clearly separated exothermic peaks are observed; this indicates that during the transformation two principal crystalline phases appear. One can see that the peaks temperatures are higher at higher heating rates. 'The cusp-like features in the DCS scans at temperatures between 415-418°C indicate the Curie temperatures Tc. These values are close to the result by Harmlin et al. of Tc= 413.3 °C [12].
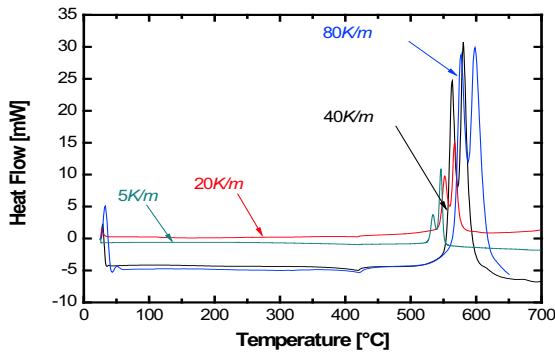
Fig. 1. DSC thermograms of the as-cast $Fe_{78}Si_9B_{13}$ metallic glass at heating rates of 5, 20, 40 and 80 K/min.

Differential scanning calorimetry (DSC) measurements of thermally treated and annealed samples at 420°C are presented in figure 2. One can observe from the DSC curve of the sample annealed at 420°C for 8h that only the second crystallization appears. Thus it explains that at this annealing time, the first stage of crystallization have been achieved completely. Figure 2 presents the continuous crystallization process and shows the fully crystallized structure without any transition observed in DSC measurement. However, the DSC curve in fully sample presents a solid-state phase transformation that is not reversible (not reported here).The kinetics indicates that during transformations two crystallization steps appear in table 1. The first crystallization temperatures observed in the thermograms are moved towards higher values with the increasing annealing time.
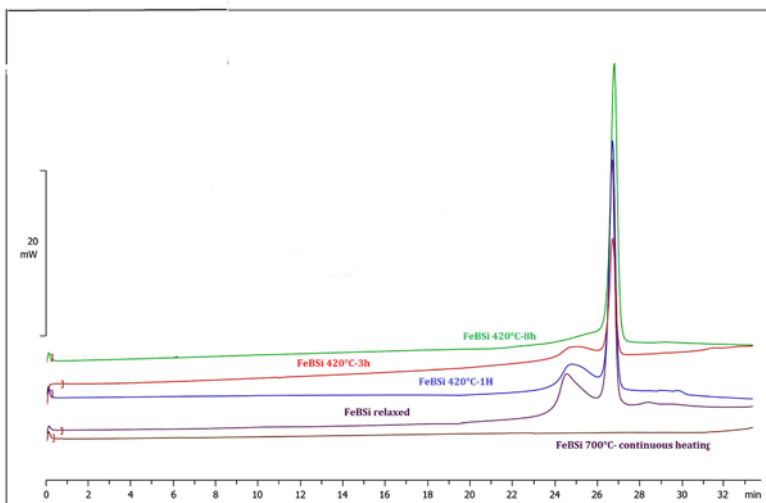

Fig. 2. DSC thermograms of the annealed at 420°C and continuous heated $Fe_{78}Si_9B_{13}$ samples.

3.2 Analysis of kinetics

These phase transformations may be assumed to be thermally activated processes. For thermally activated processes the heating rate β and the peak temperatures T_p are linked by the following equation:

$$\beta = \beta_0 \exp(-E_a / R.T_p). \tag{1}$$

β_0 is the pre-exponential factor,
R: the gas constant and
E_a: the apparent activation energy.

The results for activation energies and pre-exponential factors of the two crystallization events observed in the DSC plots are summarized in table 1.

Table 1. Parameters describing the crystallization kinetics for all studied samples

Sample	E_a (T_1) kJ/mole	β_1 K/s	$E_A(T_2)$	β_2 K/s
As quenched	384	5,9867 10^{23}	308	4,2779 10^{18}
Relaxed	311	1,2096 10^{20}	304	2,7550 10^{18}
420°C/1H	295	7,9441 10^{18}	315	1,8718 10^{19}
420°C/3H	203	5.91 10^{12}	314	1,5588 10^{19}
420°C/8H	---	---	296	1,3627 10^{18}

Based on Kissinger's model, the activation energy of crystallization can be derived from:
$$\ln(\beta / T_P^2) = E_c / R T_p + \text{Constant} \tag{2}$$

Figure 3 shows the plots of $\ln(\beta / T_P^2)$ against $1000/T_p$. We can use the slope of the fitted data to calculate the activation energy E_c. Then the Kissinger analysis of the DSC scans gives the parameters compiled in table 2.
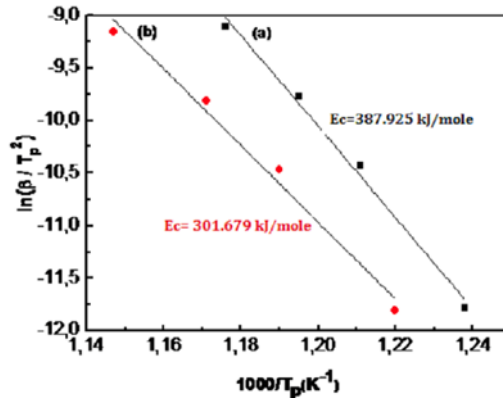

Fig. 3. $\ln(\beta/T_p^2)$ versus $1000/T_p$ plot for $Fe_{78}Si_9B_{13}$ metallic glass: (a) first peak and (b) second peak. Solid lines correspond to linear fit of the experimental data

Table 2. Values of activation energies E_{c1} and E_{c2} calculated by Kissinger's model for the Fe$_{78}$Si$_9$B$_{13}$ metallic glass.

Activation energy E_{c1} for the first crystallization stage (kJmol^{-1})	**357.925**
Activation energy E_{c1} for the second crystallization stage (kJmol^{-1})	**301.679**

By comparison, the Auguis-Bennet's model describes the kinetics by using Equation 3 to calculate the activation energy E_c of the crystallization as well as the frequency factor K_0.

$$\ln(\beta/T_p) = -E_c/RT_p + \ln(K_0) \tag{3}$$

The figure 4 and the table 3 describe the deduction of E_c and K_0 with the same procedure previously used. Since the Fe-Si grains determine the magnetic properties of the material, the study of the first peak is interesting. So, the apparent activation energy according to thermally activated process was deducted (E_{c1} = 384 KJ mol^{-1}) and agrees with a kinetic evaluation of the peak temperature according to Kissinger's and Auguis-Bennet's models [13-14]. More kinetic analysis can be described using different models like The Advance Model Free Kinetics (AMFK) model developed by Vyazovkin [15-16]. Results of kinetics for relaxed and annealed samples give further information concerning the crystallization process. It should be noted that the activation energy changes fundamentally during crystallization.
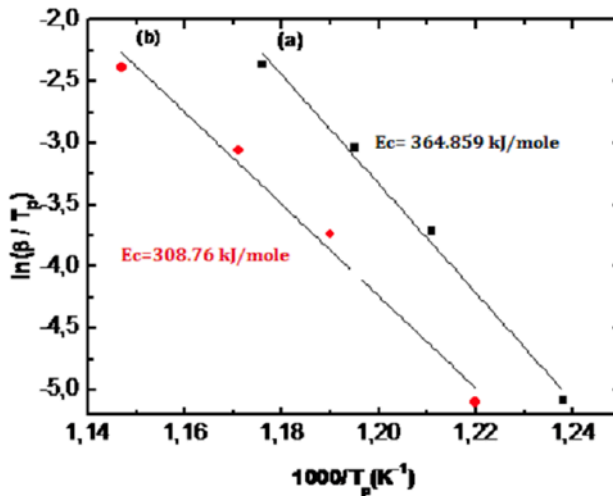

Fig. 4. $\ln(\beta/T_p)$ versus $1000/T_p$ plot for Fe$_{78}$Si$_9$B$_{13}$ metallic glass (a) first peak and (b) second peak. Solid lines correspond to linear function fit of experimental data

Table 3. Values of activation energies, E_{c1} and E_{c2}, calculated by Auguis-Bennet's model for the $Fe_{78}Si_9B_{13}$ metallic glass.

Activation energy E_{c1} for the first crystallization stage (kJmol^{-1})	**364.859**
Activation energy E_{c1} for the second crystallization stage (kJmol^{-1})	**308.76**
Frequency factor K_0	**lnK_0**
	49.348

3.3 X-Ray Diffraction results

Indeed, we are speaking of amorphous ribbons. We then stated that the samples are "partially crystalline". This can be contradictory. In reality, the ribbons exhibit, as we shall see with the X-ray diffraction, a small outgrowth indicating an appearance of α- Fe crystallites. The as-purchased material is a relaxed amorphous ribbon that contains some amounts of α-Fe of bcc structure whose (110) line emerges over the stretched amorphous halo. This demonstrates that the heat treatment slightly modified the structure which is not completely amorphous (see fig.5a).

The following annealing treatments on samples from the relaxed ribbon induce an increase of the amount of the α-Fe of bcc structure from the residual amorphous phase with the formation of borides.

The X-rays diffraction patterns (XRD) of the annealed ribbons show, in fig.5b, the main lines belong to bcc solid solution α-(Fe, Si) and tetragonal Fe_3B. The proportions of the crystalline phases related to the X-rays intensity indicate a different amount of phases within the different samples. At 420°C-1H, a (110) α–Fe peak corresponding to d_{hkl} at about 2.02 nm on the XRD spectrum can be observed along with a small peak of (301) tetragonal (t) Fe_3B at d_{hkl} = 2.33 nm. This latter increases following the annealing time. Moreover, the 2.02 nm peak shows a side peak at about 2.01 nm which is likely that of (121) of t-Fe_2B. However in the XRD spectrum of the sample heated to 700°C, the intensity of the peak at 2.02 nm is greater than that of the peak at 2.33 nm without any additionnal peak of t-Fe_2B. These observations indicate that the proportion of the α–Fe is greater in the sample heated than in the annealing samples. Thus long annealing time favours the borides formation.
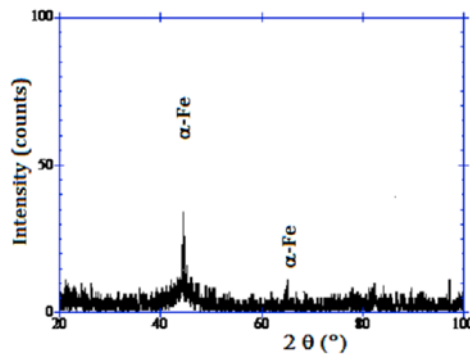
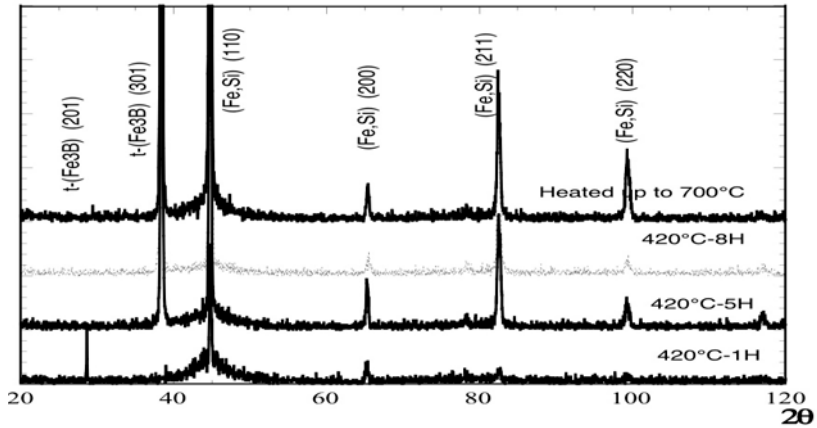**Fig. 5a.** XRD pattern of relaxed ribbon

Fig. 5b. XRD patterns of crystallized $Fe_{78}Si_9B_{13}$ ribbons after annealing at 420°C for 1, 5, 8, hours, and for aribbon continuously heated up to 700°C.

3.4 Magnetic properties

We performed two separate experiments over time with the same samples. The first, to evaluate the saturation magnetization at high magnetic field and to confirm the role of the increase of the α–(Fe-Si) phase in the annealed material. Figure 6 shows the magnetization of annealed samples as a function of the applied magnetic field up 2 tesla (20000 Oersted). Progression to complete saturation seems faster for samples annealed during 5h and 8h with a tendency to unidirectional anisotropy. For the relaxed (amorphous) sample, the saturation is more difficult to achieve and is reached beyond the maximum applied field , this suggests that saturation is facilitated with the increase of volume fraction of the α-(Fe,Si) phase. For the relaxed sample, the structural relaxation may cause the value of the saturation relatively low compared to the treated samples from 5h to 8h when the soft magnetic phase (Fe, Si) is present in more large quantities.

In order to better define the remarkable properties of this soft magnetic material, we use a lower magnetic field experiment using a fluxmeter. Coercivity and anisotropy could be deduced from the hysteresis cycles for all samples. For a good comparison, as-cast amorphous samples show a low coercivity H_c and a fairly high magnetization with a low magnetocrystalline anisotropy indicating a rounded cycle characteristic of the amorphous structure.

An annealing procedure without applied magnetic field makes a somewhat rounded appearance. In this case, two processes are present: domain wall movement and rotation of moments.
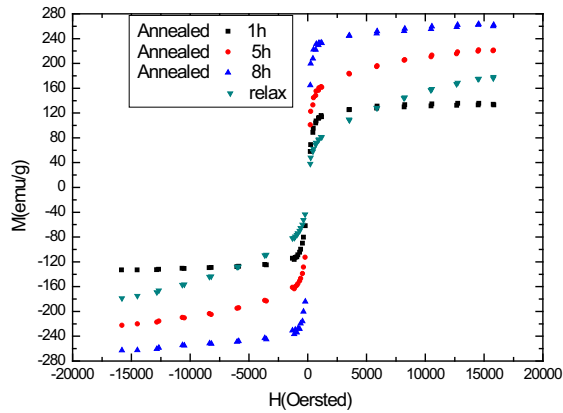
Fig. 6. Magnetization of annealed samples as a function of the applied magnetic field up 2 tesla

Table 4 presents some characteristic values inferred from hysteresis loops for maximum applied magnetic field H_{max}=1 kOe (VSM) giving magnetization M_s and hysteresis loops up to 27000 A/m (about 300 Oe) give the coercive field and relative anisotropy.

The amorphous Fe-Si-B alloys which are treated at 420°C for 1 hour remain amorphous. Structural relaxation takes place due to the formation of Fe_3Si, which is a soft magnetic phase. For the annealed alloys, we observe a strong increase in coercivity for the Fe-Si-B alloy with the annealing time. The growth of dendrites increases the coercivity by providing additional obstacles for the movement of the domain walls. In addition, the formation of hard magnetic phase Fe_3B results in a deterioration of soft magnetic properties. Indeed, the formation of the Fe_3B phase leads to an increase in the magneto-crystalline anisotropy, following which the magnetic curing takes place. For longer annealing times up to 8 hours, the saturation magnetization continues to increase due to the formation of the Fe_3Si phase. The Fe_3B phase continues to increase in parallel. When the sample is brought to 700 ° C, the magnetization continues to increase for the Fe-Si-B alloy due to the stopping of Fe_3B evolution as well as the (Fe,Si) phase progression (see section 3.3). Thus, the anisotropy decreases due to the reduction of the influence of the Fe_3B phase which no longer progresses.

Conclusion

We have studied the thermal behavior of amorphous and thermally treated $Fe_{78}B_{13}Si_9$ ribbons that contain a certain amount of bcc-αFe. DSC and XRD were used. Pre-annealed samples were annealed at 420°C during 1, 3, 5 and 8 hours.

The kinetics indicates that during transformations two crystallization steps appear.

XRD diffraction confirmed the presence of the latter phase and the stability of the bcc-α-Fe crystals due to the crystallization of the residual amorphous phase during the increase of the heating time.

Magnetic measurements indicate an evolution by annealing procedure which suggests improvement of saturation magnetization and occurring of directional anisotropy characterized by a growing remnant magnetization, but also destroying of mechanical properties as ductility and leads to magnetic hardening by increasing of coercive field H_c.

Table 4. Some properties inferred from hysteresis loops measured for the different samples by VSM and fluxmeter

Sample	Ms (emu/g) at 1 kOe VSM	Mr (emu/g) at 1kOe VSM	Hc (A/m) at 300 Oe Fluxmeter	Mr/Ms at 300 Oe Fluxmeter	Hc/Mr at 300 Oe Fluxmeter
As cast 1	116.89	4.13	22	0.0350	5.327
As cast 2	102.83	4.72	25	0.0459	5.297
Relaxed	51.415	17.884	460.834	0.348	25.773
1h	46.12	15.28	541.381	0.331	35.461
3h	124.575	52.519	602.44	0.422	11.479
5h	undefined	undefined	730.105	0.230	
8h	89.226	31.712	882.369	0.355	27.778
700°C	105.341	50.45	989.896	0.475	19.607

References

[1] Y. Tong, B.Z Ding. H.G. Jiang, K. Lu, J.T.Wang and Z.Q. .Hu, J. Appl. Phys., **75**, 1 (1994)

[2] R. Hasegawa, Applications of amorphous magnetic alloys, Material Science and Engineering A, **A375-377**, 90-7 (2004)

[3] M.-A. Escobar, A. Reza Yavari, R. Barrue and J.C. Perron, IEEE Trans. Magn. 2, **4**, 1911-1916 (1992).

[4] Hang Nam Ok and A.H. Morrish, Phys. Rev. B, **22**, 3471-3480 (1980).

[5] H. Sakamoto, T. Yamada, N. Okumura, T. Sato, Mater. Sci. Eng. **A 206**,150-153 (1996).

[6] H. Chiriac and C. Hison, , J. Mag. Mater. **254-255,** 475-476 (2003)

[7] F. Luborsky, in *Amorphous Metallic Alloys*, (*ed.* F.E. Luborsky, Butherworth, London, 1983) p.360

[8] E.P. Wolfarth, *in Amorphous Metallic Alloys*, (ed. F.E. Luborsky Butherworth, London, 1983) p.283.

[9] H. Kronmüller, Phil. Mag. **B48**, 127 (1983)

[10] P.A.Pankhurst, J.Z. Jiang, S. Betteridge, M.R.J. Gibbs, G.A.Gehring, J. Phys-Condens. Mat., **7**, 957 (1995)

[11] T. Kulik, H.T. Savage, and A. Hernando, J. Appl. Phys. 73, 10 (1993)

[12] M.Harmelin, E. Etchessahar, J. Debuigne and J. Bigot, Thermochimica Acta, **130**, 177-192 (1988)

[13] H. E. Kissinger, Anal. Chem. **29**, 1702 (1994).

[14] J.A. Augis, J. E. Bennet, J. Therm. Anal. **13**, 283 (1978)

[15] S.Vyazovkin , Thermochem. Acta, **194,** 375-383 (1992).

[16] S.Vyazovkin and C. A.Wight, Annu. Rev. Phys. Chem, **48,**125-149 (1997).